

Modification of FAO Penman–Monteith equation for minor components of energy

Arman Varmaghani, William E. Eichinger and John H. Prueger

ABSTRACT

The conventional Food and Agriculture Organization of the United Nations (FAO) Penman–Monteith (P-M) equation requires knowledge of the available energy to estimate reference evapotranspiration (ET_o); however, it is common to ignore the minor energy components (MECs). This study was conducted to determine the effect of not including the MECs in the FAO P-M equation. Fifteen-min micrometeorological records of four sites (covered with corn, soybeans, and prairie) in central Iowa, USA, during the years 2007–2012 were investigated. The major/minor components of the energy equation were either measured or estimated by *in-situ* eddy covariance instruments. It was discovered that, on average, the MECs accounted for at least 13% of daily net radiation, leading to 27% decrease in daily ET_o . Therefore, an equation is introduced to estimate MECs as a function of net radiation, air temperature, and Monin–Obukhov length; and another equation is regressed to roughly estimate daily MECs as a function of net radiation and day of the year. The findings in this study suggest a fundamental modification of FAO P-M formula by considering the inclusion of MECs in the energy term.

Key words | crop coefficient method, FAO Penman–Monteith, minor energy components, reference evapotranspiration

Arman Varmaghani (corresponding author)
William E. Eichinger
 IIHR – Hydrosience & Engineering,
 The University of Iowa,
 100 C. Maxwell Stanley Hydraulics Laboratory,
 Iowa City, IA 52242-1585,
 USA
 E-mail: arman.varmaghani@gmail.com

John H. Prueger
 USDA (United States Department of Agriculture),
 ARS (Agricultural Research Service),
 2110 University Blvd, Ames, IA 50011,
 USA

INTRODUCTION

Evapotranspiration (ET) is a term used to describe water loss from the surface of the Earth to the atmosphere. It includes the process of evaporation of liquid water from water bodies and soil, etc. and transpiration from vegetation. The importance of ET has been revealed in a variety of scientific fields. As a controlling factor governing how the sun's energy will be partitioned into latent and sensible heat, ET is an important variable in atmospheric transport and the water cycle, and hence plays a key role in meteorology, hydrology, and agriculture. The amount of ET depends upon the availability of water at the surface, the amount of available energy (required to change the phase of the water, known as latent heat of evaporation, LE), the ability of the atmosphere to accommodate water vapor (i.e. vapor pressure deficit (VPD)), and a mechanism for water transport from the land surface to the atmosphere (mainly

through turbulent transport). Net radiation, R_n , is the main source of energy, and wind-generated turbulence is generally the transport mechanism.

One of the well-established convenient models of ET estimation, adopted by the United Nations Food and Agriculture Organization (FAO 2015), is the crop coefficient method (Allen *et al.* 1998), where the ET of each crop is related to a reference ET (ET_o) by a dynamic crop coefficient (K_c):

$$ET = K_c ET_o \quad (1)$$

K_c is a function of land cover, the growth stage of the plant, soil characteristics, and available water in both the top-soil and root zone. ET_o is the ET of a hypothetical reference crop with specific static characteristics (specifically, a well-watered, 0.12 m grass with an albedo of 0.23 and an aerodynamic surface resistance of 70 s m^{-1}). It is

estimated from the well-known FAO Penman–Monteith (P-M) equation:

$$ET_o = \frac{0.408\Delta(R_n - G) + \gamma \frac{900}{T_a} U_2(VPD)}{\Delta + \gamma(1 + 0.34U_2)} \quad (2)$$

where Δ is the slope of the saturation vapor pressure vs. temperature curve [kPa K^{-1}]; G is ground heat flux [$\text{MJ m}^{-2} \text{day}^{-1}$]; γ is the psychrometric constant [kPa K^{-1}] which is a function of air pressure (P); U_2 represents wind velocity at 2 m above the displacement height [m s^{-1}]; VPD is in [kPa]; and ET_o will be rendered in [mm day^{-1}] (FAO 2015). The term $(R_n - G)$ in the equation is the available energy (part of the surface energy balance) in a coupled land–atmosphere system, and it is given by:

$$R_n = LE + H + G \quad (3)$$

where H stands for sensible heat flux (Brutsaert 1982), while the minor components of energy (MECs) in the derivation of the P-M equation are customarily ignored (TCRM 2016). MECs consist mainly of, but are not limited to, the energy required for photosynthesis, heat storage in the soil, canopy and air, advection, and snow thaw. It has been known for more than three decades that direct measurements of the elements of Equation (3) suffer from lack of closure (Leuning *et al.* 1982; Bolle *et al.* 1995; Oncley *et al.* 2007; Foken 2008). The significance of the energy imbalance arises from the fact that the accuracy of a model is linked to the accuracy of its validation measurements. Global climate and regional models, to a great extent, are dependent upon the energy partitioning of the surface of the planet. The lack of closure impacts the methodologies used to map evapotranspiration as the residual of the energy balance equation (Foken 1998; Li *et al.* 2009).

There are three primary causes for energy imbalance: measurement errors, the nonidentical elevations of these measurements, and the elimination of ‘insignificant’ components (i.e. MECs) contributing to the energy equation (Foken 2008). If the contributions of these MECs turn out to be significant in ET estimation, the FAO P-M equation should be modified accordingly. These terms that researchers generally presumed to be negligible may turn out to be

significant under certain circumstances, such as storage terms (Oliphant *et al.* 2004; Jacobs *et al.* 2008; Moderow *et al.* 2009; Lindroth *et al.* 2010), or the advection term (Aubinet *et al.* 2010; Kochendorfer & Paw 2011), which can account for as much as 10% of the imbalance in the energy budget (Oncley *et al.* 2007). Even though the contribution of MECs can be significant under certain circumstances, there is no research including these terms in the FAO P-M equation. Therefore, the objectives of this paper are to: (a) investigate the significance of MECs for ET estimation by FAO P-M equation based on analyzing six years’ records of *in-situ* micrometeorological measurements of four Iowan sites; and (b) explore the possibility of estimating MECs based on major energy components and available variables. The article will begin with an explanation of the data exploited in this study.

STUDY AREA AND DATA

This work supports the Iowa Flood Center’s (<http://iowa-floodcenter.org/>) development of a flood warning system, where spatially resolved daily ET over Iowa is required by the model. Iowa is mostly cloudy: the city of Des Moines, IA, for example, reports a total number of only 105 sunny days, including the days with a cloud cover of at most 30% (Osborn 2015). The State is categorized as zone 2 according to AIA Climate Zones, a cold weather with less than 2,000 CDD (cooling degree days) and greater than 7,000 HDD (heating degree days) (RECS 2005); summers are hot and humid, with daytime temperatures sometimes near 32 °C. Average winters in the State have been known to drop well below freezing, even dropping below –28 °C. Analysis of land cover Cropland Data Layer (CDL) maps provided by National Agricultural Statistics Service (NASS 2015) shows that 80% of Iowa is covered by corn, soybeans, and prairie. Accordingly, we investigated four sites as being typical of Iowa and their specifications are reflected in Table 1. Sites #1, 2, and 3 were adjacent farms, and site #4 was 57 km away from them. The sites were of rectangular shape. Sites #1–3 were switched from corn to soybeans in an irregular fashion and shape each year. These sites are long-term sites maintained by the USDA National Laboratory for Agriculture and Environment (NLAE) with high-quality,

Table 1 | Specifications of the sites used in this study

#	Site ID	Latitude/longitude/altitude	Land cover*	Dimension
1	Brooks10	41°58"29.7696" N 93°41"26.1024" W +314	Corn/Soybeans	437 × 760 m
2	Brooks11	41°58"28.1928" N 93°41"37.3704" W +315	Corn/Soybeans	487 × 1,536 m
3	BeenofIowa	41°59"01.9860" N 93°40"56.7480" W +315	Corn/Soybeans	816 × 1,630 m
4	NSP_prairie	41°33"31.0356" N 93°17"34.3104" W +279	Prairie	1,500 × 3,100 m

*Land cover code 'Corn/Soybeans' indicates the annual rotation.

well-maintained equipment (ARS 2015). We have recorded data for these agricultural fields quasi-continuously every 15 minutes since 2006, with minimal gaps due to field activities (i.e. planting), periodic calibrations, and sensor or data-logging problems. The annual precipitation in Iowa amounts to 889 mm, while the year 2012 was an exceptional drought year with 660 mm precipitation. Therefore, we selectively focused on the time series between the years 2007 and 2012. Due to data gaps, a total of 171,089 15-min data points (~20% of the entire period), and a total of 4,911 daily data points (~56% of the entire period) were left for analysis.

We exploited 13 variables measured by *in-situ* instruments to estimate the required energy fluxes and ET_o . The list of these variables along with the specification of instruments are reflected in Table 2. We computed turbulent fluxes of H , LE , and momentum from the micrometeorological sensors using

an EC system operating at 20 Hz. The raw data were processed using software developed at the USDA ARS. R_n was measured by a pyranometer, and the temperature–humidity sensors contained thin-film platinum resistance thermometers thermally attached to a capacitive relative humidity (RH) sensor. Two soil heat flux plates (SHFPs) were buried at each site, one exactly below the vegetation row and the other between the rows. The depth of the SHFPs changed each year for different fields. We buried four soil thermocouples: two above each of the SHFPs were co-located and their elevation varied annually at 2, 4, and 6 cm below ground. Infrared gas analyzers (IRGAs) were open path sensors. All devices were wired to a Campbell Scientific CR3000 data logger, and powered with deep cycle marine batteries connected to solar panels. An in-depth procedure to estimate the energy components is covered in Varmaghani et al. (2016).

Table 2 | Specification of the instrumentation used in the study

Instrument	Model	Variable(s) ^a	Height ^b
3D sonic anemometer	Campbell Scientific CSAT3	U , LE , H , P	1.8–5.2 m
Infrared gas analyzer	LI-COR 7500	CO_2	0.84–5 m
HMP45C	PRT	T_a	1.55–5.3 m
Humidity probe	Honeywell HIH – 4602C	RH	1.55–5.3 m
Infrared sensor	IRPT-P3 (Apogee Inc.)	T_s , T_c	0.84–5 m
Pyranometer	Kipp and Zonen CM21	R_n	1.4–6.1 m
SHF plate	HFT – 3.1	SHF ^c	6, 8, 10 cm
Soil thermocouple	Campbell Scientific 107-L	SoilTC ^c	2, 4, 6 cm
Soil moisture probe	Hydra 50 Hz	Hydra_V ^c	5 cm

^a U is wind component; LE , H , and SHF represent latent, sensible, and soil heat flux, respectively; T_a , T_s , and T_c denote air, surface, and above-canopy temperature, in order; RH stands for relative humidity; R_n is net radiation; SoilTC and Hydra_V represent soil temperature and probe's voltage.

^bHeights varied typically year-by-year, site-by-site, and in summer/winter period, and are above-ground measurements.

^cDenotes measurements of same variable at different locations.

METHODOLOGY

Since Equation (3) is the simplified version of the energy balance equation by ignoring MECs, the complete form of this equation (Brutsaert 1982) can be written as:

$$R_n = H + LE + SHF + S_g + S_a + S_c + F + A + \chi \quad (4)$$

where S_g , S_a , and S_c , in order, represent heat storage between the SHFP and the surface, heat storage in the air, and canopy; and F denotes photosynthesis where CO_2 flux is used as an indicator. SHF stands for soil heat flux at the plate; given the fact that plates are buried in the ground, some energy is always stored between the plate and surface (S_g), and G will be calculated from algebraic summation of SHF and S_g . A is the advection term, and χ represents other terms, which mainly include freeze/thaw in a snow-pack, and soil water transport (Higgins 2012). Rewriting Equation (4) according to measurements from eddy covariance (EC) towers, and we shall have the unbalanced energy equation:

$$\underline{R_n} \neq \underline{H} + \underline{LE} + \underline{SHF} + \underline{S_g} + \underline{S_a} + \underline{S_c} + \underline{F} + \underline{A} + \chi + \varepsilon \quad (5)$$

where the underlined symbol for each variable indicates measurement from an *in-situ* instrument, and ε represents systematic measurement errors.

As with all measurements, these are subject to uncertainty and what appears to be a systematic bias. Surface measurements of \underline{LE} and \underline{H} are systematically underestimated (Leuning et al. 1982; Bolle et al. 1993; Oncley et al. 2007; Foken 2008). In order to adjust the fluxes and rectify the major/minor components of energy, an *a posteriori* analysis by means of constrained linear multiple regression can be conducted. *A posteriori* analysis methodology (Higgins 2012) basically brings balance to the energy equation (namely, Equation (5)) in a least-squares fashion, and identifies the degree of responsibility of each component for lack of energy balance closure. *A posteriori* analysis does not close the energy equation without the contributions of MECs. In other words, even after flux adjustment, Equation (5) is closed while Equation (3) may still suffer from lack of closure (imbalance). We denote

this amount of imbalance by E_m henceforth, and it can be formulated as follows:

$$E_m = R_n - (H + LE + G) = S_a + S_c + F + A + \chi \quad (6)$$

where the variables represent the true values of energy components wherein the adjusted energy components are used instead. The parameter S_g is embedded in G . The term E_m accounts for the loss of energy due to ignoring MECs, chiefly heat storage, photosynthesis, and advection. If the contributions of MECs to the available energy turn out to be significant, the FAO P-M equation should be modified as follows:

$$ET_{om} = \frac{0.408\Delta(R_n - G - E_m) + \gamma \frac{900}{T_a} U_2(VPD)}{\Delta + \gamma(1 + 0.34U_2)} \quad (7)$$

where ET_{om} represents ET_o when MECs are considered.

RESULT AND DISCUSSION

We previously estimated all of the underlined variables in Equation (5) over the Iowan sites. Then, we adjusted the energy components based on an *a posteriori* analysis by means of constrained linear multiple regression (refer to Varmaghani et al. (2016) for details). An example of this correction is shown in Figure 1 for major fluxes. The figure illustrates the daily-averaged measurements of major fluxes vs. the adjusted ones over the Iowan sites for the years 2007–2012. The underlined variables in the X-axes denote *in-situ* measurements in Equation (5) while the Y-axes are the adjusted ones except that the Y-axes in subplots (a) and (b) represent the difference between the two fluxes. The subplots confirm that the latent and sensible heat fluxes are mainly underestimated while the most reliable measurement is usually attributed to R_n (Foken 2008). According to the subplots, as the absolute value of fluxes increases, the associated uncertainty in estimation tends to increase. The ratio of the adjusted flux over the measured flux, r , for these daily-averaged R_n , G , LE , and H were 0.98, 0.93, 1.20, and 1.34, respectively. This indicates that R_n , and G were rather overestimated.

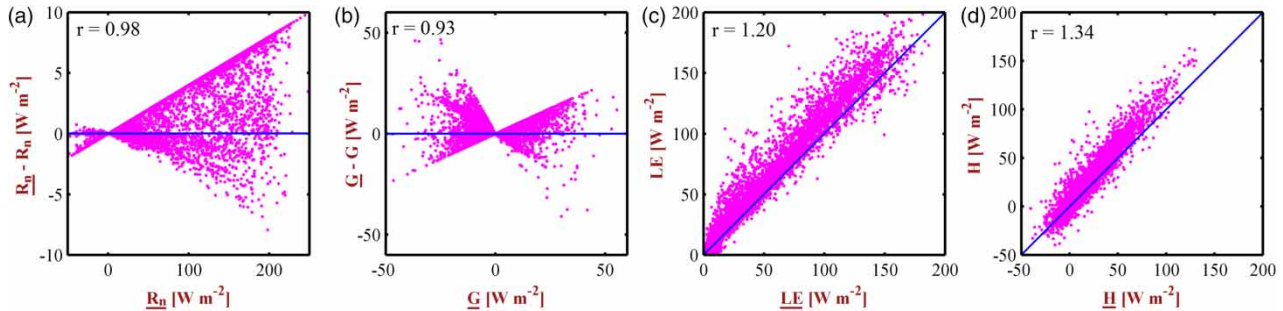


Figure 1 | Daily-averaged *in-situ* measurements of major fluxes (X-axis) vs. adjusted ones (Y-axis) over the Iowan sites for the years 2007–2012. The Y-axis in subplots (a) and (b), however, represents the difference between the two fluxes. The underlined symbol denotes *in-situ* measurement. r denotes the average ratio of the flux adjusted over the *in-situ* flux. A total number of 6,326, 5,496, 6,658, and 5,120 daily-averaged data points for R_n , G , LE , and H , respectively.

As discussed earlier, when the fluxes are adjusted, Equation (4) will be closed while Equation (3) still suffers from lack of closure, and the term E_m should be estimated. Therefore, we calculated the term E_m over the four Iowan sites according to Equation (6) separately for each crop for the years 2007–2012. Figure 2(a) depicts the daily variation of E_m as a fraction of R_n for different crops throughout the year. It was expected that E_m should be commensurate with R_n . As can be seen, the contribution of MECs during the peak growing season is minimum (~13%), confirmed by Meyers & Hollinger (2004), and maximum E_m occurs during winter (~35%). There is no noticeable difference between the E_m trend of various crops. Figure 2(b) demonstrates the variation of E_m/R_n as a function of day of the year and hour of the day. The white colors indicate nonexistence of data; there are two opposite white bows (one at the mid-top (sunset) and one

at the mid-bottom (sunrise) devoid of the term E_m/R_n since R_n approaches zero, and the atmosphere goes to the neutral phase. Except for the mentioned bows, there are no other trends observable in subplot (b).

In order to observe the influence of the term E_m in ET_o estimation, and subsequently in ET estimation, ET_o was computed from Equation (2) and from Equation (7). The computations were performed at 15-min temporal scale, and then summed up to daily. Figure 3 aptly illustrates the difference between these two values on a daily basis. It is clear from the subplots that the ET_o over corn and soybeans is subject to more correction than over prairie. Typically, corn shows higher correction (ET_{om} is 31% less than ET_o), and this percentage for soybeans and prairie is about 29 and 20%, sequentially. On average, the ET_{om} is 27% less than common ET_o , which indicates the importance of considering MECs in ET_o computation and consequently in

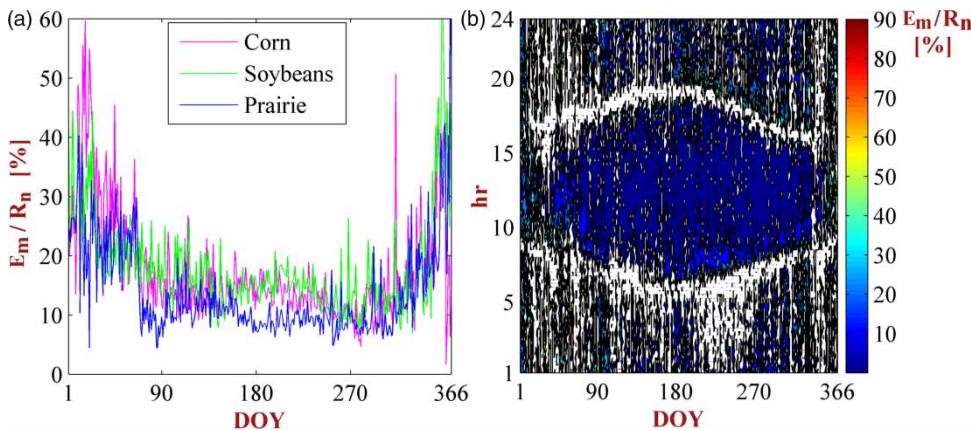


Figure 2 | (a) Daily variation of the term E_m as a fraction of R_n for various crops throughout the year. (b) Variation of E_m/R_n as a function of day of the year and hour of the day. The data were for the years 2007–2012. DOY stands for day of the year and hr denotes hour.

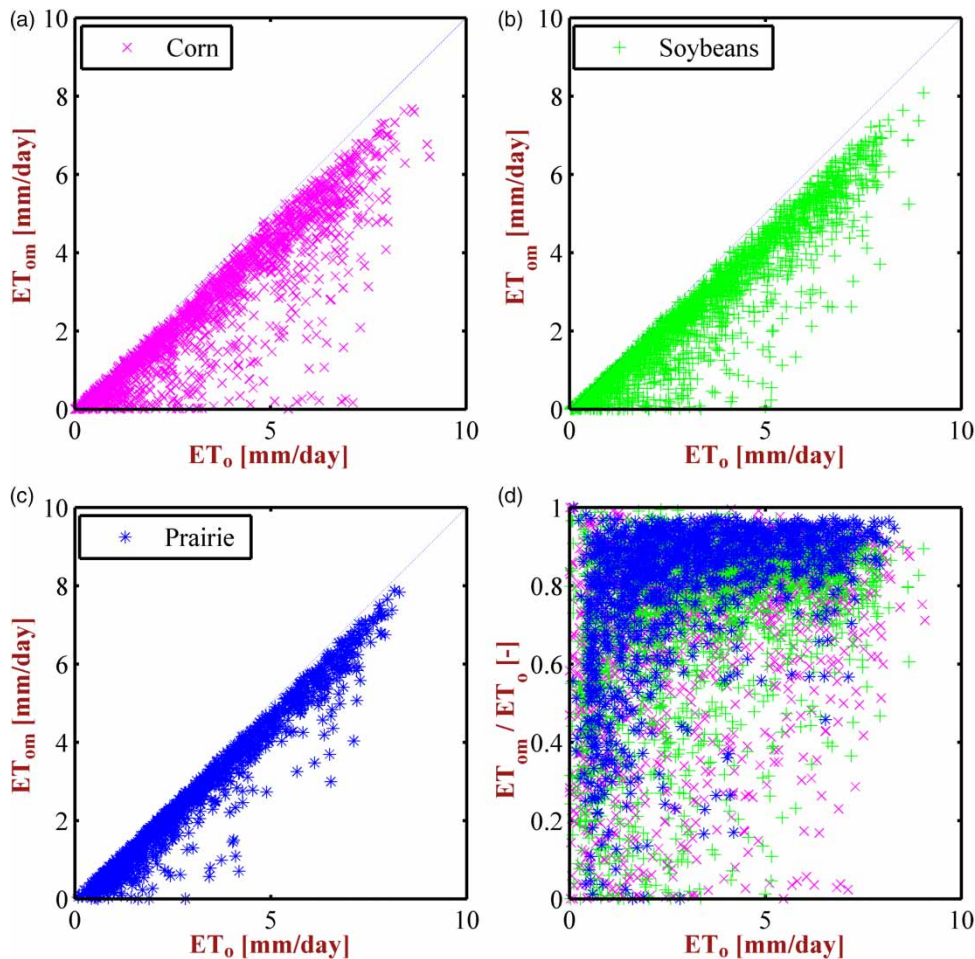


Figure 3 | (a)–(c) Scatter plot of $ET_{o,m}$ vs. ET_o in $[\text{mm day}^{-1}]$ for corn, soybeans, and prairie, respectively. (d) Scatter plot of $ET_{o,m}/ET_o$ vs. ET_o in $[\text{mm day}^{-1}]$ for three vegetation types, records of four lowland sites during the years 2007–2012; total number of 1,695, 1,953, and 1,263 daily records for corn, soybeans, and prairie, in order.

ET estimations. Figure 3(d) depicts the ratio $ET_{o,m}/ET_o$ vs. ET_o for different crops.

Adjustment of major/minor components of energy are pre-requisite to estimate the E_m term, implying that the knowledge of these components is required; however, with regard to large-scale ET estimation in practical applications, not only is the quantification of MECs not possible, but also estimation of the major components of energy is challenging (Li *et al.* 2009). The only available energy component in the P-M equation is R_n , and G is commonly calculated as a portion of R_n in an indirect way (Norman *et al.* 1995). Therefore, an estimation of the term E_m is highly desirable.

We investigated the possibility of introducing E_m as a function of available variables (i.e. R_n , T_a , RH , P , U_2 , LE ,

G , and H), and the only fully developed pattern is illustrated in Figure 4 for each crop separately (subplots (a)–(c)) and for the combination of the three vegetation types (subplot (d)). The results are based on 15-min records where the surfaces in the figure are smoothed by a moving average block of 5×5 . As the figure explains, the term E_m (as a percentage of R_n) can be estimated as a function of air temperature and Monin–Obukhov length (L) which describes the effect of buoyancy on turbulent flows. L is also an indicator of advection of energy (Higgins 2012). Furthermore, it is generally used as an indicator of atmosphere stability ($L < 0$, $L = 0$, and $L > 0$, respectively for unstable, neutral, and stable phase), and can be represented as a function of friction velocity (u_*), latent, and sensible heat

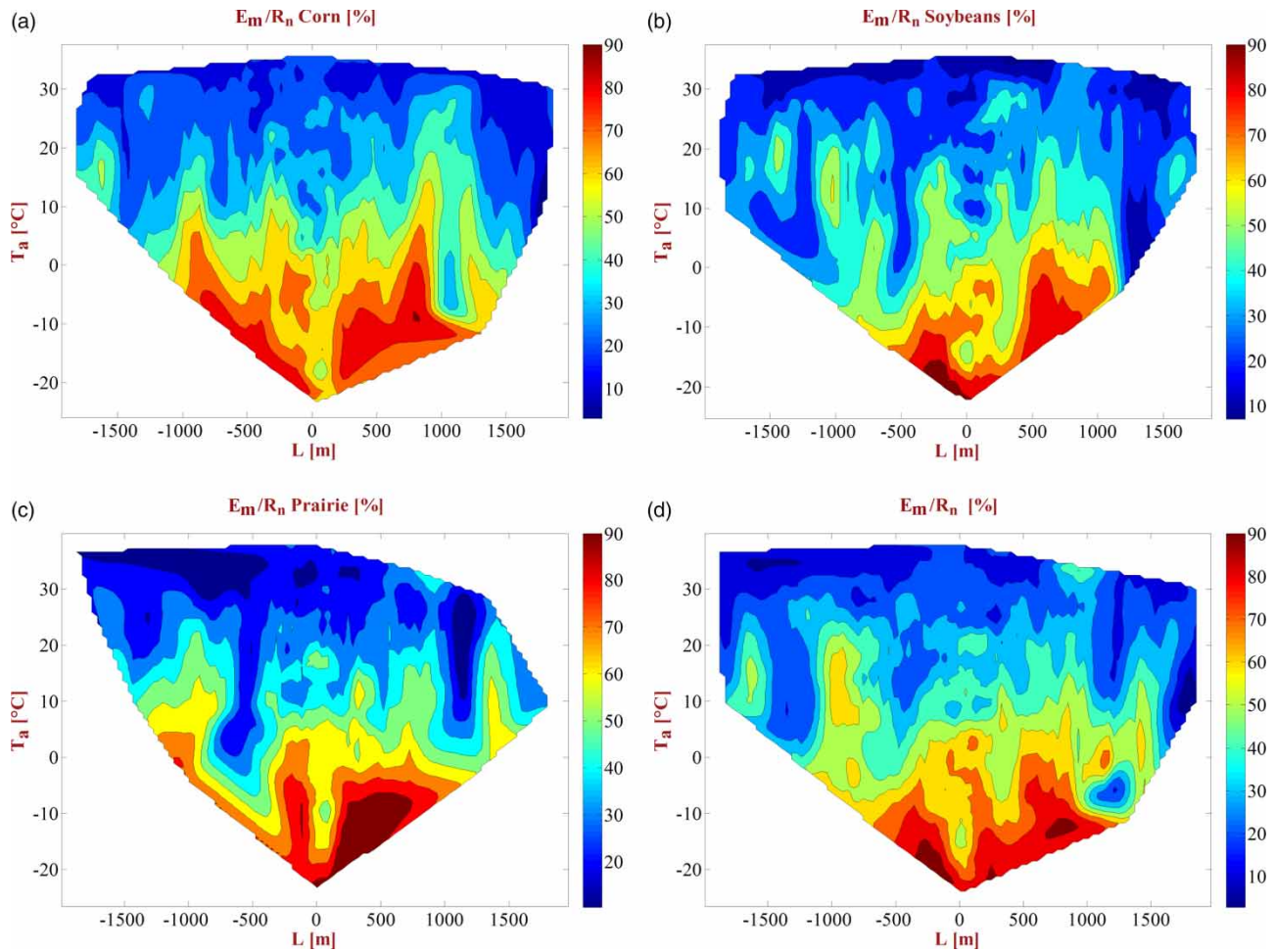


Figure 4 | Variation of E_m (as a fraction of R_n) [%] as a function of L and T_a . (a)–(c) pertain to corn (64,184 data points), soybeans (67,308 data points), and prairie (39,597 data points), respectively. (d) The variation of E_m for the combination of the three vegetation types (171,089 data points).

flux:

$$L = \frac{-u_z^3 \rho_a}{g\kappa \left(\frac{H}{T_a C_p} + 0.61 \frac{LE}{L_e} \right)} \quad (8)$$

where ρ_a denotes density of air; and g , κ , and L_e represent acceleration due to gravity, Von-Karman constant, and latent heat of vaporization, sequentially (Brutsaert 1982). As Figure 4 indicates, the three vegetation types show similar patterns, and the subplot (d) can be solely used for estimation of E_m over the three vegetation covers. Therefore, the subsequent equation was fitted to Figure 4(d):

$$E_m = [-0.00509|L| - 1.178T_a + 61.77]R_n \quad (9)$$

where the root mean squared error (RMSE) was 8.96% and the adjusted coefficient of determination (R^2) was determined to be 0.81. The equation was regressed over the 15-min records of the four Iowan sites. If the friction velocity can somehow be estimated, a recursive solution of Equations (1), (6), (7), (8), and (9) will lead to estimation of the term E_m given the fact that $ET = LE \times L_e$.

Meso-scale estimation of friction (shear) velocity is challenging due to lack of required variables. The Global Modelling Assimilation Office (GMAO) of NASA provides numerous hydrometeorological variables including shear velocity with temporal resolution of 1 hour (GMAO 2015); however, the spatial resolution is coarse (~ 22 km). Since the conventional meteorological stations rarely provide friction velocity (e.g. RWIS (2016)), the following formula with

RMSE = 4.7% and $R^2 = 0.60$ was additionally fitted to the average of the curves in Figure 2(a):

$$E_m \approx \left[0.13 + 1.91 \times 10^{-10} \left(\text{DOY} - \frac{366}{2} \right)^4 \right] R_n \quad (10)$$

where DOY stands for day of year, and E_m is represented as a fraction of R_n on a daily basis. Equation (10) approximates the term E_m (rough estimation) at daily scale for the three vegetation types over the Iowan sites.

CONCLUSION

In this paper, four Iowan sites during the years 2007–2012 were investigated. The EC towers, installed in the middle of the farms (namely corn, soybeans, and prairie), provided 15-min records of micrometeorological variables. The major/minor components of energy had been previously adjusted due to lack of closure, and finally the term E_m was calculated. The annual variation of E_m (Figure 2) showed that the term E_m is minimum (~13% of R_n) during the peak growing season, and is maximum (~35% of R_n) during the winter for the three vegetation types. Figure 3 revealed that, even after flux adjustment, ignoring minor energy components, on average, can result in overestimation of daily reference ET by 27%. This indicates the importance of considering minor components of energy in reference ET computation and consequently in ET estimations. The regression among the potential variables (Figure 4) demonstrated that the minor energy components can be indirectly estimated as a function of net radiation, air temperature, and Monin–Obukhov length (Equation (9)) in a recursive solution. This was expected since the Monin–Obukhov length is an indicator of advection of energy (Varmaghani et al. 2016), and balance of energy between latent and sensible heat fluxes (Equation (8)). Since the three selected vegetation covers showed similar patterns (Figure 4), we hypothesize that similar patterns will be found in other vegetation types, and the term E_m as a function of net radiation, air temperature, and Monin–Obukhov length can be generalized. Since meso-scale estimation of friction (shear) velocity is challenging, it is suggested to

pay particular attention to its mapping as future research. This issue led the authors to introduce Equation (10) for rough estimation of daily E_m as a function of net radiation and day of the year in the absence of friction velocity. The result in this study indicated that the FAO Penman–Monteith equation (namely, the reference ET equation) needs to be modified by considering the minor energy components in its energy term. Since the majority of ET models apply the simplified version of the energy balance equation (i.e. Equation (3)) to estimate ET as the residual of the energy equation (Li et al. 2009), the findings in this study strongly urge that ignoring the minor components of energy should be done with caution, and these energy balance ET models may require investigation of the importance of the proposed equations in their validation.

ACKNOWLEDGEMENTS

This work was accomplished under the grant support of Iowa Flood Center (<http://iowafloodcenter.org/>). We are grateful to the USDA National Laboratory for Agriculture and Environment (NLAE), Ames, IA for providing the micrometeorological data. Cropland Data Layer maps were provided by National Agricultural Statistics Service of USDA, Washington DC, USA. We also express our appreciation to the anonymous reviewers for their constructive remarks.

REFERENCES

- Allen, R. G., Pereira, L. S., Raes, D. & Smith, M. 1998 *Crop Evapotranspiration-Guidelines for Computing Crop Water Requirements*. FAO Irrigation and Drainage Paper 56. FAO, Rome, Italy, 300 pp.
- ARS 2015 *Agricultural Research Service, National Laboratory for Agriculture and the Environment*. From http://www.ars.usda.gov/main/site_main.htm?modecode=50-30-15-00 (accessed 4 May, 2015).
- Aubinet, M., Feigenwinter, C., Heinesch, B., Bernhofer, C., Canepa, E., Lindroth, A., Montagnani, L., Rebmann, C., Sedlak, P. & Van Gorsel, E. 2010 *Direct advection measurements do not help to solve the night-time CO₂ closure problem: evidence from three different forests*. *Agricultural and Forest Meteorology* **150** (5), 655–664.

- Bolle, H.-J., Andre, J.-C., Arrue, J., Barth, H., Bessemoulin, P., Brasa, A., De Bruin, H. A. R., Cruces, J., Dugdale, G. & Engman, E. 1995 EFEDA – European field experiment in a desertification-threatened area. *Annales Geophysicae* **11**, 173–189.
- Brutsaert, W. 1982 *Evaporation Into the Atmosphere: Theory, History, and Applications*. Reidel, Dordrecht, The Netherlands.
- FAO 2015 *Chapter 2 - FAO Penman-Monteith Equation*. <http://www.fao.org/docrep/x0490e/x0490e06.htm> (accessed 19 August, 2015).
- Foken, T. 1998 Die scheinbar ungeschlossene Energiebilanz am Erdboden-eine Herausforderung an die Experimentelle Meteorologie. *Sitzungsberichte der Leibniz-Sozietät* **24** (5), 131–150.
- Foken, T. 2008 *The energy balance closure problem: an overview*. *Ecological Applications* **18** (6), 1351–1367.
- GMAO 2015 *Global Modeling and Assimilation Office, NASA*. <http://gmao.gsfc.nasa.gov/>.
- Higgins, C. W. 2012 *A-posteriori analysis of surface energy budget closure to determine missed energy pathways*. *Geophysical Research Letters* **39** (19), 1–5.
- Jacobs, A. F., Heusinkveld, B. G. & Holtslag, A. A. 2008 *Towards closing the surface energy budget of a mid-latitude grassland*. *Boundary-layer Meteorology* **126** (1), 125–136.
- Kochendorfer, J. & Paw, U. K. T. 2011 *Field estimates of scalar advection across a canopy edge*. *Agricultural and Forest Meteorology* **151** (5), 585–594.
- Leuning, R., Denmead, O., Lang, A. & Ohtaki, E. 1982 *Effects of heat and water vapor transport on eddy covariance measurement of CO₂ fluxes*. *Boundary-layer Meteorology* **23** (2), 209–222.
- Li, Z. L., Tang, R., Wan, Z., Bi, Y., Zhou, C., Tang, B., Yan, G. & Zhang, X. 2009 *A review of current methodologies for regional evapotranspiration estimation from remotely sensed data*. *Sensors* **9** (5), 3801–3853.
- Lindroth, A., Mölder, M. & Lagergren, F. 2010 *Heat storage in forest biomass improves energy balance closure*. *Biogeosciences* **7** (1), 301–313.
- Meyers, T. P. & Hollinger, S. E. 2004 *An assessment of storage terms in the surface energy balance of maize and soybean*. *Agricultural and Forest Meteorology* **125** (1), 105–115.
- Moderow, U., Aubinet, M., Feigenwinter, C., Kolle, O., Lindroth, A., Mölder, M. & Bernhofer, C. 2009 *Available energy and energy balance closure at four coniferous forest sites across Europe*. *Theoretical and Applied Climatology* **98** (3–4), 397–412.
- NASS 2015 *State Crop Progress and Condition*. http://www.nass.usda.gov/Publications/State_Crop_Progress_and_Condition/ (accessed 25 April, 2014).
- Norman, J. M., Kustas, W. P. & Humes, K. S. 1995 *Source approach for estimating soil and vegetation energy fluxes in observations of directional radiometric surface temperature*. *Agricultural and Forest Meteorology* **77** (3), 263–293.
- Oliphant, A., Grimmond, C., Zutter, H., Schmid, H., Su, H.-B., Scott, S., Offerle, B. J. C. R., Randolph, J. C. & Ehman, J. 2004 *Heat storage and energy balance fluxes for a temperate deciduous forest*. *Agricultural and Forest Meteorology* **126** (3), 185–201.
- Oncley, S. P., Foken, T., Vogt, R., Kohsiek, W., DeBruin, H., Bernhofer, C., Christen, A., van Gorsel, E., Grantz, D. & Feigenwinter, C. 2007 *The energy balance experiment EBEX-2000. Part I: overview and energy balance*. *Boundary-layer Meteorology* **123** (1), 1–28.
- Osborn, L. 2015 *Days of Sunshine per Year in Iowa*. <http://www.currentresults.com/Weather/Iowa/annual-days-of-sunshine.php> (accessed 10 April, 2015).
- RECS 2005 *AIA Climate Zones, Residential Energy Consumption Survey*. <https://www.eia.gov/consumption/residential/maps.php> (accessed 10 April, 2017).
- RWIS 2016 *Road Weather Information System (RWIS)*. <http://www.ops.fhwa.dot.gov/weather/faq.htm> (accessed 18 August, 2016).
- TCRM 2016 *Derivation of the Penman–Monteith equation*. In: *Task Committee on Revision of Manual, Evaporation, Evapotranspiration, and Irrigation Water Requirements*, Vol. 70, 2nd edn (TCRM, ed.). ASCE, Reston, VA, pp. 619–625.
- Varmaghani, A., Eichinger, W. E. & Prueger, J. H. 2016 *A diagnostic approach towards the causes of energy balance closure problem*. *Open Journal of Modern Hydrology* **6** (2), 101.

First received 25 June 2018; accepted in revised form 27 October 2018. Available online 7 December 2018